



- 1 Lacustrine methane release on the Tibetan Plateau as an
- 2 important driver of Early Miocene global warming
- 4 Cheng Yang 1,2,3, Xiugen Fu 1,2,3,4\*, Jinxian Deng 1,2,3\*, Hengye Wei 1,2,3, Yue Wen 1,2,3,
- 5 Tianxiang Wen<sup>1,2,3</sup>, Shengqiang Zeng<sup>5\*</sup>
- 6 <sup>1</sup> School of Geoscience and Technology, Southwest Petroleum University, Chengdu
- 7 610500, China

- 8 <sup>2</sup> State Key Laboratory of Oil and Gas Reservoir Geologyand Exploitation, Southwest
- 9 Petroleum University, Chengdu
- 10 610500, China
- 11 <sup>3</sup> Qiangtang institute of Sedimentary Basin, Southwest Petroleum University, Chengdu
- 12 610500, China
- 13 <sup>4</sup> Qinghai Provincial Key Laboratory of Plateau Saline-Lacustrine Basinal Oil & Gas
- 14 Geology, Dunhuang
- 15 736202, China
- 16 5 Chengdu Center, China Geological Survey (Geosciences Innovation Center of
- 17 Southwest China), Chengdu 610218, China
- \*Correspondence to: Xiugen Fu (fuxiugen@126.com), Jinxian Deng (448920726@qq.com),
- 19 Shengqiang Zeng (zengsq@126.com)
- 20 Address: School of Geoscience and Technology, Southwest Petroleum University, Chengdu,
- 21 610500, China

22

https://doi.org/10.5194/egusphere-2025-5342 Preprint. Discussion started: 27 November 2025 © Author(s) 2025. CC BY 4.0 License.





23 Abstract. The Early Miocene was a key period of significant global warming. While 24 previous studies often attributed this warming to the India-Asia collision and associated 25 volcanism, an alternative mechanism may involve large-scale methane release from organic-rich lake sediments. To test the hypothesis that methane emissions from Tibetan 26 27 Plateau lakes contributed to Early Miocene warming, we analyzed organic carbon, stable isotopes, and elemental concentrations in samples from the organic-rich 28 29 Dingqinghu Formation in the Lunpola Basin, central Tibetan Plateau. Our results identify an exceptionally strong positive carbonate carbon isotope excursion (δ<sup>13</sup>C<sub>carb</sub> 30 31 up to +13.79‰) within the lacustrine deposits. The large carbon isotope difference 32 between carbonate and organic matter ( $\Delta^{13}C > 32\%$ ) indicates that methanogenesis, 33 specifically via acetate fermentation, was the dominant microbial process. Extremely 34 low sulfur contents likely suppressed sulfate-driven anaerobic oxidation of methane, 35 facilitating direct methane release to the atmosphere. Furthermore, volcanic activity 36 during this interval was limited, suggesting a negligible role in carbon cycle 37 perturbations. The close temporal correspondence between Early Miocene warming, 38 rising atmospheric CO2, and methane emissions documented on the Tibetan Plateau 39 indicates that methane release from these plateau lakes may have played an important 40 role in driving global warming and increasing contemporary CO<sub>2</sub> levels.

41





### 1 Introduction

42

43 The Cenozoic era witnessed several global warming episodes, such the Paleocene-44 Eocene Thermal Maximum and the Middle Miocene Climatic Optimum, with 45 temperatures and atmospheric CO2 concentrations significantly exceeding preindustrial levels (Methner et al., 2020; Cenozoic CO2 Proxy Integration Project 46 47 (CenCO2PIP) Consortium, 2023; Ivany et al., 2025). This period was also defined by 48 continental collision between India and Eurasia and the subsequent uplift of the Tibetan 49 Plateau, a tectonic event that profoundly reshaped Asian climate and potentially 50 influenced global patterns (Wang et al., 2008; Yang et al., 2022; Zhang et al., 2024; Zhang 51 et al., 2025). The temporal coincidence of these events has led to the hypothesis that the 52 India-Asia collision and its associated volcanism may have been a primary driver of 53 Cenozoic warming (Gutjahr et al., 2017; Kender et al., 2021; Tremblin et al., 2022).

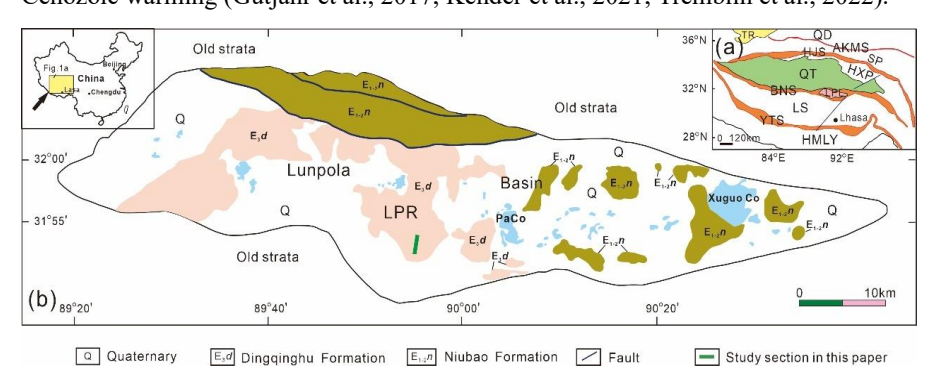


Figure 1:(a) Map of the Tibetan plateau showing major terranes. (b) Simplified geological map of the

Lunpola Basin, showing location of sampling section. AKMS, Anyimaqen–Kunlun–Muztagh Suture;

57 BNS, Bangong Lake-Nujiang River Suture; HJS, Hoh Xil-Jinsha River Suture; HMLY, Himalayas;

58 HXP, Hoh Xili piedmont zone; LPL, Lunpola Basin; LS, Lhasa terrane; QD, Qaidam; QT, Qiagtang

Basin; SP, Songpan-Ganzi flysch complex; TR, Tarim Basin; YTS, Yarlung Tsangpo Suture (modified

60 from Fu et al,2015).

54

59

However, Cenozoic volcanism on the Tibetan Plateau, while episodic, was relatively

62 limited in scale (Xie et al., 2024). For instance, during the third volcanic phase (ca. 28–

63 18 Ma), activity was largely confined to restricted areas like the Lunpola Basin, with





64 significantly reduced spatial distribution and magma volume compared to earlier stages 65 (Wang et al., 2024). Consequently, although regional magmatic events reflect the 66 tectonic-magmatic evolution of the Plateau, their associated volatile fluxes were likely 67 negligible on a global scale compared to large igneous provinces (Zhang et al., 2021). 68 This suggests that the direct contribution of Tibetan volcanism to the rise in atmospheric 69 CO<sub>2</sub> and global warming was probably limited. 70 An alternative mechanism for driving warming may involve large-scale methane 71 release from organic-rich lake sediments. During diagenesis and burial, microbial 72 methanogenesis in such sediments can generate substantial methane (CH<sub>4</sub>) (Martens 73 and Berner, 1974; Whiticar, 1999; Bastviken et al., 2004; Dean et al., 2018). Under 74 stratified or anoxic lacustrine conditions, this methane can accumulate and be released 75 to atmosphere via ebullition and diffusion (Bastviken et al., 2004; Encinas Fernández 76 et al., 2014; DelSontro et al., 2016). Lakes are a significant natural source of methane 77 emissions, and during specific geological intervals, widespread organic-rich lacustrine 78 systems could have release methane at a scale capable of influencing the global climate 79 system by enhancing the greenhouse effect and perturbing the carbon cycle (Dean et al., 80 2018; Sun et al., 2022; Zhuang et al., 2023). Consequently, organic-enriched lake 81 sediments act not only a crucial long-term carbon sink but also, under certain conditions, 82 as a potent methane source, with substantial implications for both paleoclimate and 83 contemporary climate systems. 84 During the Miocene, the Tibetan Plateau hosted extensive lacustrine systems. The 85 Lunpola and Nima basins, for example, preserve thick successions of organic-rich 86 deposits and oil shales. In the Dingqinghu Formation, these successions reach thicknesses exceeding 148 m and exhibit total organic carbon (TOC) contents of up to 87 88 17.60% (Fu et al., 2012; Fang et al., 2020; Fu et al., 2020; Lu, 2023; Zeng et al., 2024). 89 These deposits not only record high organic carbon accumulation but also represent a 90 potential source of large methane emissions during deposition and early diagenesis, 91 which could have contributed to regional or even global warming (Zhou et al., 2024;





92 Nie et al., 2023). 93 To test the hypothesis that methane release from Tibetan Plateau lakes contributed to 94 Early Miocene warming, we conducted organic carbon, stable isotope, and element 95 analyses on samples from the Dingqinghu Formation in the Lunpola Basin (Fig. 1a). 96 Integrated with a robust chronological framework (Mao et al., 2019), this multi-proxy 97 dataset allows us to correlate regional geological events with global climate records and 98 evaluate the potential mechanisms driving Early Miocene climate warming. 99 Geological setting 100 The Lunpola Basin is a Cenozoic fault-depression basin located on the central Tibetan 101 Plateau, within the central segment of the Bangong-Nujiang Suture Zone (BNSZ), a 102 major tectonic boundary separating the Lhasa and Qiangtang terranes. The basin 103 extends approximately 200 km from east to west and 10-30 km from north to south, 104 and is recognized as the highest-altitude petroleum-bearing basin in the world (Deng et 105 al., 2012; Rowley & Currie, 2006; Fu et al., 2012; Wang et al., 2025). 106 The Tibetan Plateau comprises a series of east-striking tectonic units bounded by 107 major suture zones. From north to south, they are the Kunlun-Qaidam Terrane, the 108 Songpan-Ganzi flysch complex, the Qiangtang Terrane, and the Lhasa Terrane, 109 separated by the Anyimaqen-Kunlun-Muztagh, Hoh Xil-Jinsha River, and Bangong 110 Lake-Nujiang River (BNS) suture zones, respectively (Fig. 1a). The BNS originated 111 from the diachronous, west-to-east closure of the Meso-Tethyan ocean basin, 112 culminating in the Late Jurassic-Early Cretaceous Lhasa-Qiangtang collision (Kapp 113 and DeCelles, 2019). It was later reactivated during contractional events in the latest 114 Cretaceous and Oligocene-early Miocene, which led to the development of 115 intermontane basins in central Tibet, including the Lunpola, Nima, and Gerze basins 116 (e.g., Wei et al., 2017; Han et al., 2019). 117 Structurally, the basin is influenced by strike-slip and thrust faulting, forming a pod-118 like framework characterized by "north-south structural zoning and east-west fault





120 depression. The southern margin is controlled by thrust belts and uplifts, while the 121 northern part shows localized highs despite significant subsidence and thick 122 sedimentary infill. The cumulative thickness of the Niubao and Dingqinghu formations 123 exceeds 3,000 m. East-west segmentation by faults results in a pattern of peripheral 124 uplift and central subsidence (Lei et al., 1997). 125 The tectonic evolution of the Lunpola Basin involved two main stages. The Eocene 126 rifting, during which the Niubao Formation (E<sub>1-2</sub>n) was deposited, consisting mainly of 127 alluvial fan to fan-delta coarse clastics. The Oligocene depression, marked by 128 accumulation of the Dingqinghu Formation (E<sub>3</sub>d), dominated by deep lacustrine fine-129 grained mudstones and oil shales (Deng et al., 2012; Lu, 2023). The Dingqinghu 130 Formation is distributed primarily in the central and western parts of the basin, with 131 thickness varying from 300 to 1,100 m due to differential basement subsidence. It comprises greenish-gray shales, mudstones, and oil shales interbedded with thin 132 133 sandstones, interpreted as having been deposited in a low-energy, semi-deep to deep lacustrine environment under stable and strongly reducing conditions (Fu et al., 2015). 134 135 This study focuses on the middle member of the Dingqinghu Formation, which is 136 Early Miocene in age (ca.  $20.6 \pm 0.1$  Ma; Mao et al., 2019) and consists of organic-rich 137 mudstones, shales, and oil shales. These oil shale samples are dark brown to black in 138 color and contain high organic matter content. 139 Method 3 140 The study area and section location are presented in Fig. 1b. The vertical distribution 141 of samples within the section is presented in Figs. S1. A total of 63 samples were 142 collected from the Lunpola oil shale section. The average vertical sampling interval is 143 60 cm. 144 3.1 TOC analysis 145 First, grind the 10 mg rock sample into a powder with a particle size smaller than 200

mesh. Then, depending on the lithology and colour of the sample, 0.095-0.105 g of the





147 powdered rock is weighed into a crucible and placed into the container. Slowly add 10% 148 HCl along the inner wall of the container (ensuring it does not overflow the crucible 149 opening), then allow it to decarburise for over 24 hours until the reaction is complete. Remove the crucible, rinse the sample with high-purity water to wash away residual 150 151 acid, and continue washing until the rinse water is neutral. After washing, the samples 152 were dried in an electric thermostatic drying oven at 60-80°C and then analysed for 153 TOC content using an LDH CS analyser (Model: TK851-6K) at the Qiangtang Institute 154 of Sedimentary Basin, Southwest Petroleum University. For every 10 samples, a 155 parallel sample was included for quality control. Results were recorded in wt%, with 156 an analytical accuracy better than  $\pm 0.1\%$ . 157 Inorganic carbon and oxygen isotope analysis 158 Carbon isotope samples were analysed in the laboratory of the Qiangtang Institute of 159 Sedimentary Basin. First, an appropriate amount of carbonate sample was ground with 160 an agate mortar to less than 200 mesh, then dried in an oven at 60°C for approximately 161 4 hours to remove adsorbed water. Then, approximately 1 mg of the sample was placed 162 into the sample tube of the GasBench Plus sample preparation system. The sample was 163 dried at 70°C, the tube was sealed, and the air in the sample tube was purged with highpurity helium (He). Using an acid pump with an acid needle, excess 100% phosphoric 164 acid (H<sub>3</sub>PO<sub>4</sub>) was added to the sample tube. The phosphoric acid was allowed to react 165 166 with the carbonate sample to produce CO<sub>2</sub> gas. The generated CO<sub>2</sub> was then carried by high-purity helium into the Delta Q (Thermo Fisher) system, where the carbon and 167 oxygen isotopic compositions were measured. A standard reference material was 168 analysed after every 12 samples for quality control. Results were reported in  $\delta^{13}$ C V-169 170 PDB and δ<sup>18</sup>O V-PDB values relative to the PDB standard. The GB04416 carbonate 171 standard yielded  $\delta^{13}C = 1.67 \pm 0.05\%$ , and measurement accuracy was  $\pm 0.05\%$ . 172 For carbonate samples, analytical reproducibility of replicate standards was better than 173  $\pm 0.07\%_0$ .

176

177

178

179

180

181

182

183

184

185

186

187

188

189

190

191

192

193

194





174 3.3 Organic carbon isotope analysis

The whole rock powder sample was decarbonised with 10% HCl for 48 hours to eliminate all carbonate components, then washed with ultra-pure water until neutral, and the residual sample was dried, ground to less than 200 mesh, weighed 0.2 to 5 mg of residual powder sample into a tin cup, and tightly wrapped into cubes. Under the He atmosphere, the gas is sent into the high-temperature oxidation tube through the EA auto-sampler and instantly oxidised at 980°C in an oxygen atmosphere to generate a mixture of various gas components such as NO, N<sub>2</sub>O<sub>2</sub>, N<sub>2</sub>O<sub>2</sub>, N<sub>2</sub>, CO, CO<sub>2</sub>, H<sub>2</sub>O, SO<sub>2</sub> and halogen. In the reaction tube, CO is oxidised to CO<sub>2</sub> by chromium oxide and silvercoated cobalt oxide, and SO2 and halogen gases are removed. Subsequently, in a reduction tube at 650°C, copper wire reduces nitrogen oxides to N<sub>2</sub> and absorbs excess O2. The resulting helium and carbon dioxide gases pass through a magnesium perchlorate chemical trap to remove moisture, and then are separated by a chromatographic column into N<sub>2</sub> and CO<sub>2</sub>, which enter a thermal conductivity detector (TCD) to determine the carbon content. A small amount of CO<sub>2</sub> is then introduced into a connected Delta Q mass spectrometer via a continuous flow ConFIV system to measure the isotope ratio. All carbon isotope values are reported in the conventional  $\delta$ -notation in per mil relative to V-PDB (Vienna-PDB). The accuracy and reproducibility of the analysis were checked through repeated tests of the international standard sample USGS40, and the accuracy  $(1\sigma)$  was less than 0.09\%. The repeatability test accuracy of the sample is less than 0.13\%0.

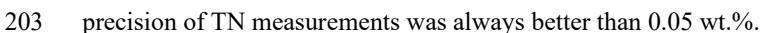
195 3.4 Total nitrogen (TN) and nitrogen isotope ( $\delta^{15}N$ )

The total nitrogen (TN) and nitrogen isotope (δ<sup>15</sup>N) contents of samples were measured at Qiangtang Institute of Sedimentary Basin, Southwest Petroleum University, China, using a Vario Macro Cube elemental analyser (Elementar, Hanau, Germany). Approximately 200 mg of the powder samples were weighed, and then add 50 mg of WO<sub>3</sub> oxidant. The mixture was tightly enclosed with a 35 × 35 mm tin capsule and prepared for analysis. Standard deviations for carbon, nitrogen and sulfur contents are





<0.05 wt% (1 $\sigma$ ) based on replicate analyses of multiple samples. Thus, the analytical



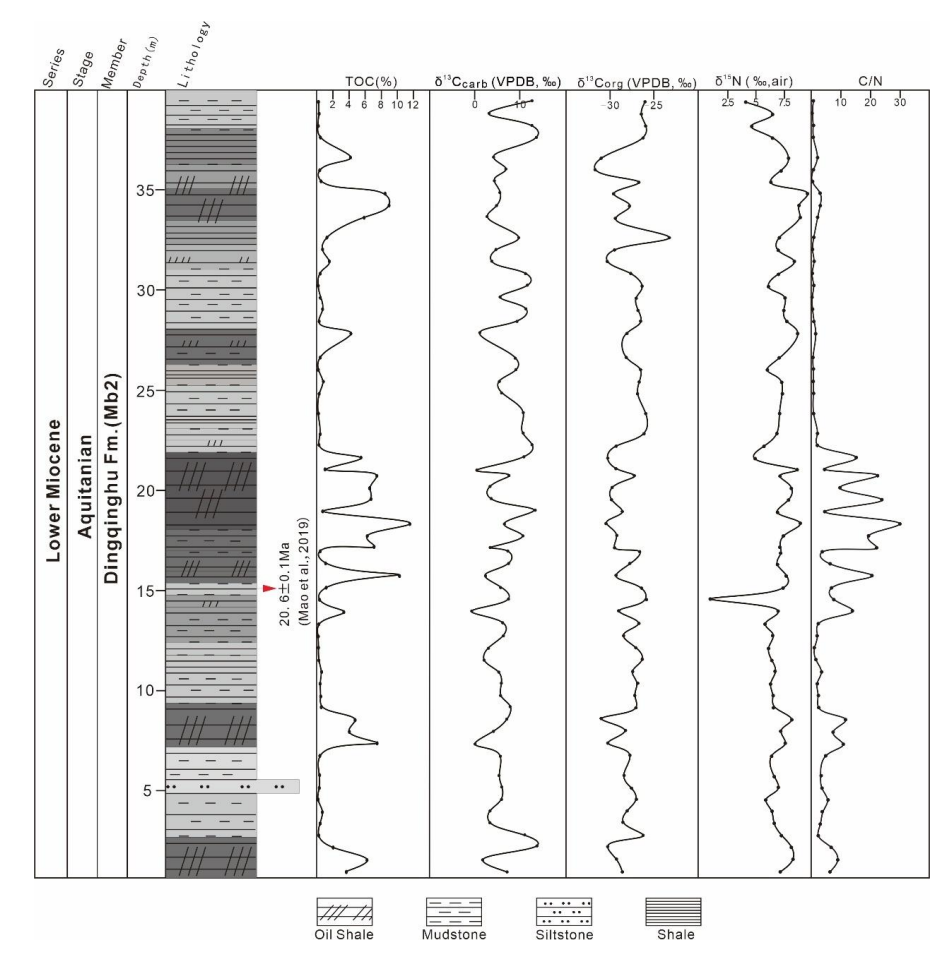


Figure 2: TOC,  $\delta^{13}C_{carb}$  (the Carbonate carbon isotope),  $\delta^{13}C_{org}$  (the Organic Carbon Isotope),  $\delta^{15}N$  (the Organic Nitrogen isotope) and C/N ratio data in Dingqinghu Formation of lunpola basin.

## 3.5 The major elements and trace elements

204

205206

207

208

209

210

211

212

Elemental analyses were conducted at the Qiangtang Basin Research Institute, Southwest Petroleum University. Powdered samples (<200 mesh) were packed into Chemplex cups, compacted, and sealed with polypropylene film. Major and selected trace element concentrations (including Ca, Mg, Ba, Cu, Ni, V and Sr) were measured using a Bruker S1 TITAN 800 X-ray fluorescence (XRF) spectrometer manufactured





213 by Bruker, Germany. The standard deviation for major elements was better than  $\pm$ 214 0.05%, and that for trace elements was better than  $\pm 20 \,\mu g/g$ . 215 4 Result 216 TOC content 217 The total organic carbon content of mudstone and oil shale samples from the Second 218 Member of the Dingqinghu formation is illustrated in Fig. 2. The TOC values exhibit a 219 wide variation range (0.12%-11.54%), with an average of 2.35%, categorizing these 220 strata as high-quality source rocks. Notably, the oil shale intervals demonstrate 221 exceptional organic enrichment, characterized by TOC values spanning 0.56%-11.54%, 222 with an average of 5.37%, which exceeds the threshold for effective hydrocarbon 223 generation in lacustrine systems. In contrast, the interbedded mudstones and shales 224 display comparatively lower TOC concentrations, ranging from 0.12% to 7.36%, with 225 an average of 0.91%. 226 Stable Isotope geochemistry 227 As shown in Fig. 2, the variations of  $\delta^{13}C_{carb}$  values of the second member of the Dingqinghu formation exhibit an extreme positive excursion, ranging from -0.84% to 228 13.79‰, with an average of 6.59‰. The variation curve of  $\delta^{13}C_{carb}$  values reveals that 229 230 mudstone intervals display the most pronounced positive excursion (1.23\%0-13.67\%0, 231 averaging 7.39\%), while oil shale intervals show relatively lower values (-0.84\%)- $13.79\%_0$ , averaging  $4.91\%_0$ ). The  $\delta^{13}C_{org}$  values of the Second Member of the 232 233 Dingqinghu Formation range from -31.64% to -23.31%, with an average value of -234 27.97\%. The  $\delta^{13}$ C<sub>org</sub> curve demonstrates a negative excursion in the oil shale layers, 235 where values vary between -31.03\% and -26.76\% (average: -29.34\%). In contrast, 236 the mudstone intervals exhibit a positive excursion, with a broader  $\delta^{13}C_{org}$  range of -237 31.64% to -23.31% and an average of -27.33%. The curves of  $\delta^{13}C_{carb}$  and  $\delta^{13}C_{org}$ 238 exhibit high coupling, which reflect the synergistic response mechanism of lake carbon

cycle and climate environment. The organic nitrogen isotope values ( $\delta^{15}N(\%_0,air)$ ) of





- 240 the Second Member of the Dingqinghu Formation range from 1.06‰ to 9.74‰, with
- 241 an average value of 7.11%.

#### 242 5 Discussion

#### 243 Influence of modifying factors

244 Since both carbonates and organic matter can preserve diagenetic information rather 245 than primary depositional signals after sedimentation, the influence of diagenesis must 246 be evaluated prior to interpreting the isotopic compositions. Following precipitation in 247 lake water bodies, carbonate minerals undergo a series of diagenetic alteration processes during burial, influenced by temperature and pore fluids. These processes, 248 249 including dissolution and recrystallization, can lead to isotopic re-equilibration between 250 the minerals and fluids (Boever et al., 2017; Hillaire et al., 2021; Huntington and 251 Petersen, 2023). The extent of diagenetic alteration in lacustrine sediments can be 252 assessed using carbon and oxygen isotopes of carbonate minerals. During diagenesis, 253 carbon in pore fluids is typically scarce relative to the reservoir within carbonates, 254 resulting in a rock-buffered system for carbon. Conversely, oxygen is predominantly 255 soured from pore fluids, creating a fluid-buffered system for oxygen. Consequently, 256 oxygen isotopic compositions are highly susceptible to alteration during diagenesis, 257 while carbon isotopic compositions generally remain more resistant to change (Wang, 258 2008; De Boever et al., 2017; Horacek et al., 2007; Ritter et al., 2017; Huntington and 259 Petersen, 2023). The correlation between carbonate  $\delta^{13}C_{carb}$  and  $\delta^{18}O$  values can 260 therefore be utilized to assess the degree of diagenetic influence on carbon isotopes. In the present study, the  $\delta^{13}C_{carb}$  vs.  $\delta^{18}O$  plot (Figs. S2a) exhibits a weak correlation 261 (R<sup>2</sup>=0.0132), indicating that the  $\delta^{13}C_{carb}$  values retain primary depositional signals. 262 263 Furthermore, the Mn/Sr ratio, a sensitive indicator of post-depositional alteration (Hu et al., 2023), show no significant correlation with either  $\delta^{13}$ C<sub>carb</sub> (R<sup>2</sup>=0.0012, Figs. S2b) 264 265 or  $\delta^{13}C_{org}$  (R<sup>2</sup>=0.017, Figs. S2c). These results collectively suggest a negligible 266 influence of diagenesis on the measured carbon isotopic signatures. 267





sediments. During diagenesis, microbial decomposition releases <sup>14</sup>N-enriched NH<sup>4+</sup> 268 into the pore water, resulting in <sup>15</sup>N enrichment of residual organic matter and more 269 positive <sup>15</sup>N values (Macko et al., 1987; Altabet, 1988; Lourey et al., 2003; Papineau et 270 al., 2009). Metamorphic processes similarly affect <sup>15</sup>N through thermal degradation of 271 nitrogen-rich compounds, which preferentially releases <sup>14</sup>N-enriched NH<sub>3</sub> or N<sub>2</sub>, 272 leaving residual organic matter with elevated <sup>15</sup>N values (Freudenthal et al., 2001; 273 274 Lehmann et al., 2002; Altabet, 2006; Robinson et al., 2012; Stüeken et al., 2016; Xia et al., 2022). Correlative relationships among TOC, TN,  $\delta^{13}C_{org}$  and  $\delta^{15}N$  serve as key 275 276 indicators for assessing post-depositional alteration. In the present study, we observe no significant correlations between  $\delta^{15}N$  and TOC (Figs. S2d), TN (Figs. S2e), C/N 277 278 (Figs. S2f), or  $\delta^{13}C_{org}$  (Figs. S2g). This demonstrates the  $\delta^{15}N$  values retain primary 279 depositional signals without diagenetic or metamorphic overprinting (Kipp et al., 2018; 280 Mettam et al., 2019). 281 Regarding terrigenous influences, lacustrine systems with substantial terrigenous 282 inputs typically exhibit  $\delta^{15}N$  values significantly lower than autochthonous algal 283 organic matter (+5% to +10%), as terrigenous organic materials (e.g., plant debris, soil 284 humus) generally show lower  $\delta^{15}$ N values (-2‰ to +5‰) (Talbot, 2002; Shen et al., 2006). While a  $\delta^{15}N_{org}$ -C/N correlation typically indicates terrestrial influence, its 285 286 absence in our dataset (Figs. S2f) confirms the  $\delta^{15}N_{org}$  values are unaffected by 287 terrigenous input. 288 Early Miocene positive carbon isotope excursion and methane release 289 The pronounced positive carbonate carbon isotope excursion recorded in the 290 Dingqinghu Formation is fundamentally controlled by the fractionation mechanisms of 291 lacustrine carbonate carbon isotopes. Consequently, investigating these fractionation processes not only elucidates the drivers of extreme  $\delta^{13}C_{carb}$  excursions but also provide 292 293 critical insights into the paleolake's carbon cycle dynamics and ecosystem function 294 during this interval. Positive  $\delta^{13}C_{carb}$  excursions in lacustrine systems primarily arise 295 from isotope fractionation during three key processes: 1) Enhanced organic matter

297

298

299

300301

302

303

304

305





production and burial, 2) Methane generation and release, and 3) Evaporative  $CO_2$ , degassing in saline lakes (Michener and Lajtha, 2008; Thottathil et al., 2022). This study will systematically evaluate these mechanisms to determine their relative contributions to the observed  $\delta^{13}C_{carb}$  excursions.

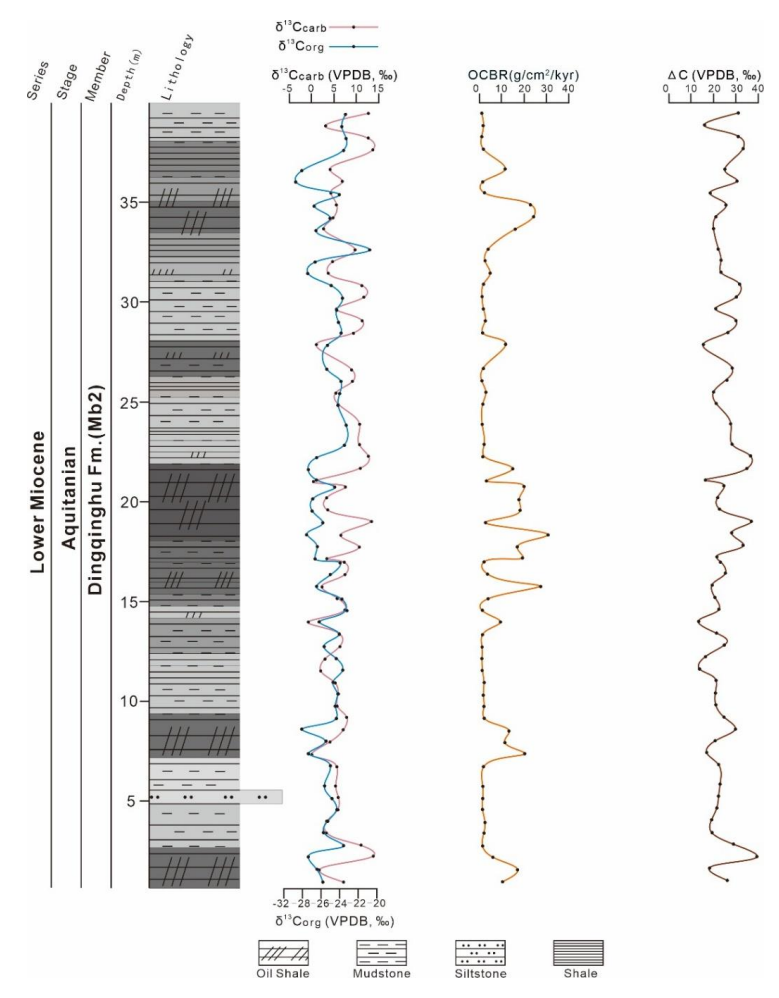


Figure 3:  $\delta^{13}C_{carb}$  (Carbonate carbon isotope),  $\delta^{13}C_{org}$  (Organic Carbon Isotope), OCBR (Organic carbon burial rate) and  $\Delta^{13}C$  value curses of Dingqinghu Formation.

## 5.2.1 Enhanced organic carbon burial

In high-productivity lacustrine systems, variations in carbonate  $\delta^{13}$ C values are predominantly controlled by lacustrine productivity (Teranes and McKenzie,





1999; Teranes and Bernasconi, 2005; Zhu, 2013). This relationship arises from 306 307 photosynthetic fractionation because aquatic plants preferentially assimilate <sup>12</sup>C when utilizing CO2 and bicarbonate from dissolved inorganic carbon (DIC) pools. This 308 309 process enriches residual DIC <sup>13</sup>C, leading to subsequent <sup>13</sup>C enrichment in precipitated carbonates (Schelske and Hodell, 1991; Neumann et al., 2002). Under high productivity 310 311 where aquatic plants preferentially consume dissolved CO<sub>2</sub>, the substantial  $\delta^{13}$ C difference between bicarbonate (relatively <sup>13</sup>C-enriched) and aqueous CO<sub>2</sub> (relatively 312 <sup>13</sup>C-depleted) further elevates  $\delta^{13}$ C values in both DIC and organic matter (Meyers, 313 314 1997; Hodell and Schelske, 1998; Leng and Marshall, 2004; Xu et al, 2006; Zhu et al., 315 2011). During lake eutrophication, algal blooms generate substantial organic matter while preferentially incorporating <sup>12</sup>C. Resultant water column anoxia preserves algal 316 317 biomass from decomposition, while high sedimentation rates enhance organic carbon burial. Carbonate minerals forming in these <sup>12</sup>C-depleted waters consequently exhibit 318 319 elevated δ<sup>13</sup>C values because sequestered <sup>12</sup>C remains buried rather than returning to 320 the water column (Müller and Suess, 1979; Calvert, 1987; Ingall et al., 1990; Tyson, 321 2001; Xu et al., 2004; Wang et al., 2015; Cartapanis et al., 2016; Megan et al., 2021; 322 Wang et al., 2022; Tegler et al., 2024). For the Dingqinghu Formation, the 323 W(V)/W(V+Ni) ratio (Fig. 4) indicates deposition under anoxic/reducing conditions. 324 Corresponding sedimentary facies represent semi-deep and deep lacustrine 325 environments with weak hydrodynamic conditions conducive to sediment preservation. 326 This depositional setting therefore favored efficient organic accumulation and 327 preservation. 328 Enhanced lacustrine productivity consistently drives both increased carbonate content and elevated δ<sup>13</sup>C values in organic matter (Meyers, 1997; Teranes and 329 330 McKenzie, 1999; Neumann et al., 2002; Leng and Marshall, 2004; Teranes and 331 Bernasconi, 2005; Xu et al., 2006; Lu et al., 2010). C/N values below 10 across most 332 stratigraphic intervals (Fig. 2) indicate autochthonous productivity dominated by 333 aquatic phytoplankton and algae, with negligible terrestrial input. This confirms TOC





serves as a reliable proxy for lacustrine productivity under limited external influences (Meyers, 1997; Zhu et al., 2013). Critically, intervals displaying positive  $\delta^{13}C_{carb}$  excursions exhibit extremely low TOC content (average < 1%), indicating depressed productivity. This inverse relationship demonstrates lacustrine productivity cannot explain the observed  $\delta^{13}C_{carb}$  excursions. Further supporting this interpretation, high-productivity systems typically yield elevated  $\delta^{15}N$  values through two mechanisms. Phytoplankton preferentially assimilate <sup>14</sup>N, enriching dissolved inorganic nitrogen pools in <sup>15</sup>N. Enhanced denitrification under anoxic conditions further amplifies  $\delta^{15}N$  increase in residual nitrogen (Sigman D, 2009). Our data reveal an inverse pattern where positive  $\delta^{13}C_{carb}$  excursions systematically coincide with negative  $\delta^{15}N$  shift (Fig. 2), demonstrating that the positive  $\delta^{13}C_{carb}$  excursion was not caused by enhanced productivity.

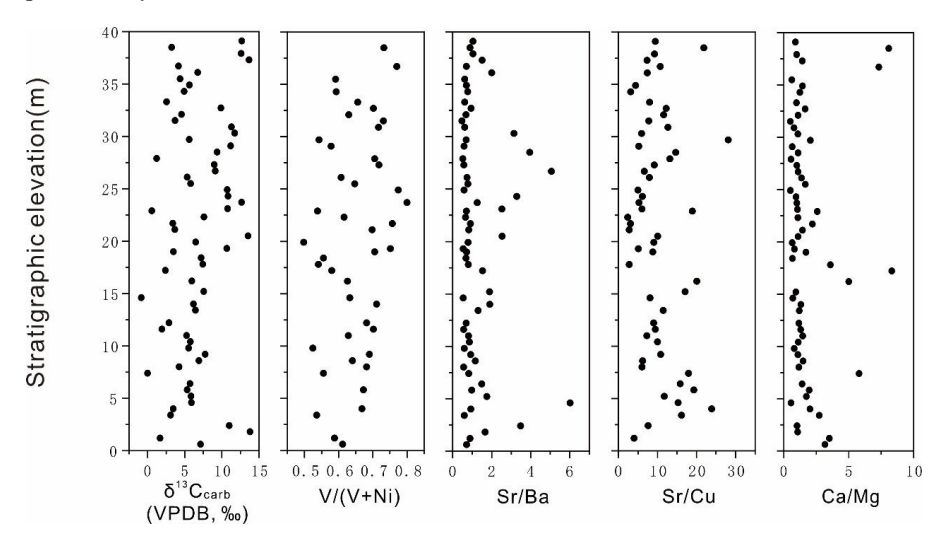


Figure 4:  $\delta^{13}C_{carb}$  (Carbonate carbon isotope), V/(V+Ni), Sr/Cu, Sr/Ba and Ca/Mg data in Dingqinghu Formation of lunpola basin.

U-Pb dating and stratigraphic thickness measurements from the Lunpori section indicate a sedimentation rate (SR) of ~107 m/Ma for the study interval of the Dingqinghu Formation (Mao et al., 2019; Xie et al., 2025). The organic carbon burial rate (OCBR) was calculated using the Eq. (1) (Shen et al., 2015):





353 OCBR  $(mg/cm^2/kyr) = SR (m/Myr) \times TOC (\%) \times \rho (g/cm^3),$ (1) 354 Assuming a bulk rock density (p) of 2.5g/cm<sup>3</sup>, OCBR values for the Dingqinghu 355 Formation in the Lunpori section were derived through unit conversion (summarized in S Table 2). Fig. 3 reveals asynchronous trends between OCBR and the positive  $\delta^{13}C_{carb}$ 356 excursion coupled with extremely low correlation coefficient. This strongly suggests 357 that variations in organic carbon burial rate were not the primary driver of the  $\delta^{13}C_{carb}$ 358 359 enrichment observed in the Dingqinghu Formation during this interval. 360 5.2.2 Evaporation 361 Strong evaporation in lakes can drive extreme positive carbonate carbon isotope values. This process promotes lake degassing, releasing CO<sub>2</sub> enriched in <sup>12</sup>C i 362 nto the atmosphere. The preferential loss of <sup>12</sup>C depletes the DIC pool in light 363 carbon, thereby increasing δ<sup>13</sup>C<sub>carb</sub> (Li and Ku, 1997; Lamb et al., 2007; Zhu e 364 t al., 2013; Boscolo-Galazzo et al., 2021). This mechanism is further supported 365 366 by studies linking evaporative salinity increase to reduced CO<sub>2</sub> solubility and k 367 inetic isotope fractionation during CO<sub>2</sub> efflux (Stiller, 1985). Consequently, arid 368 climates with intense evaporation typically elevate lake salinity and lower lake 369 levels. Palynological data from the Dingqinghu Formation (Xie et al., 2025) re 370 veal alternating dry (e.g., 21.3 Ma, 19.6 Ma) and humid phases (e.g., 20.4 Ma, 371 20.1 Ma) between 21.4 Ma and 19.4 Ma. At 20.6 Ma, pollen assemblages (Pi 372 cea, 50.1%; Pinus, 22.2%; Abies, 4.9%; and Fagaceae, 5.2%) indicate warm-hu 373 mid conditions, consistent with magnetostratigraphic cyclostratigraphic evidence 374 of dry-to-wet cycles (Su et al., 2022). Sr/Cu ratios (Fig. 4) independently confi 375 rm warm-arid to warm-humid cyclicity during deposition of the Dingqinghu Fo 376 rmation. Crucially, humid phases reduce evaporation, limiting the <sup>12</sup>C-enriched 377 CO<sub>2</sub>, and thus diminishing <sup>13</sup>C enrichment in the DIC pool. In closed basins li ke the Lunpola paleolake, evaporation intensity correlates strongly with salinity 378 (Mor et al., 2018; Han et al., 2022), making Ca/Mg ratios an effective salinity 379 380 proxy (McCormack et al., 2019; Gravina et al., 2022). However, correlation an





alyses of Ca/Mg and Sr/Ba versus  $\delta^{13}C_{carb}$  show no significant relationship bet ween salinity changes and  $\delta^{13}C_{carb}$  excursion during the Dingqinghu Formation deposition. This lack of correlation demonstrates that salinity variations did not primarily control  $\delta^{13}C_{carb}$  trend. Integrated assessment of climate proxies, salinit y indicators, and carbon isotopes indicate that while evaporation may contribute secondarily to  $\delta^{13}C_{carb}$  enrichment, it was not the principal driver of the observed positive excursion.

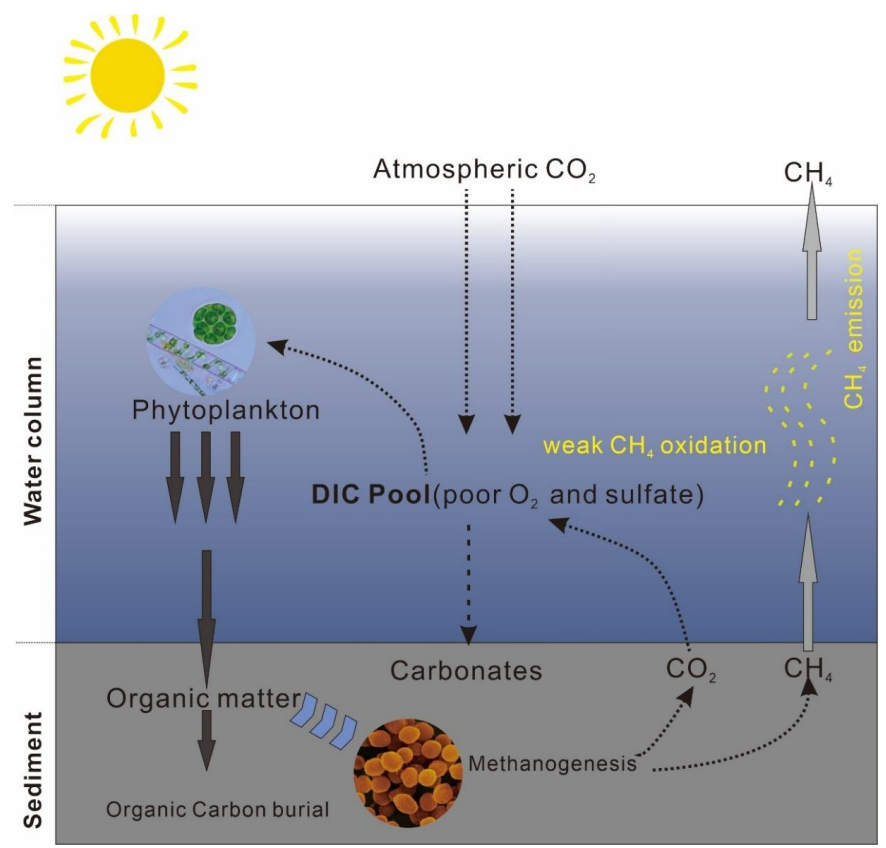


Figure 5: Schematic diagram of the carbon cycling pathway for methane release in Dingqing Lake. Biogenic methane is generated by methanogens in the anoxic sediments, and the water column is under reducing conditions, lacking electron acceptors such as sulfate and iron ions. The methane directly discharges into the atmosphere.





5.2.3 Methane release as the driver of Early Miocene positive  $\delta^{13}C_{carb}$  excursion 393 Methane generation produces significant quantities of CH<sub>4</sub> highly enriched in <sup>12</sup>C 394 alongside CO<sub>2</sub> enriched in <sup>13</sup>C. The subsequent escape of <sup>12</sup>C-enriched CH<sub>4</sub> and the 395 incorporation of <sup>13</sup>C-enriched CO<sub>2</sub> into the DIC pool drive δ<sup>13</sup>C<sub>carb</sub> enrichment in DIC-396 397 derived carbonates. Based on integrated geochemical evidence, the extreme positive excursion of  $\delta^{13}C_{carb}$  in the Dingqinghu Formation likely resulted from substantial 398 399 kinetic isotope fractionation during methanogenesis. This process facilitated the 400 preferential removal of <sup>12</sup>C as CH<sub>4</sub>, leaving the DIC pool enriched in δ<sup>13</sup>C<sub>carb</sub>. Similar mechanisms are documented in organic-rich lacustrine systems. Examples include Tilo 401 402 and Lake Bosumtwi, where methanogenesis elevated carbonate δ<sup>13</sup>C values to approximately +12% (Talbot and Kelts, 1986; Lamb et al., 2007; Rosqvist et al., 2007). 403 Methanogenesis in Lake Apopka generated pore water  $\delta^{13}$ C values up to +26.4% (Gu 404 et al., 2004), while Lake Dziani Dzaha recorded average carbonate  $\delta^{13}$ C values of +16.2 405  $\pm 1.1\%$  (Cadeau et al.,2020). In Lake Caohai, it increased lacustrine carbonate  $\delta^{13}$ C to 406 407 +20.94‰ (Zhu et al.,2013). 408 Unlike marine sediments dominated by CO<sub>2</sub>-reducing methanogenesis (Eq. (R1)), the organic-rich, reducing Lunpola paleolake during Dingqinghu Formation deposition 409 410 provided an optimal environment for bacterial fermentation. Here acetoclastic 411 methanogenesis (Eq. (R2)) prevailed as the primary methane production pathway 412 (whitticar et al., 1986). Critically, methane fate diverges significantly between marine 413 and lacustrine systems. In marine setting, methane is largely consumed at the Sulfate-414 Methane Transition Zone (SMTZ) via syntrophy between sulfate-reducing bacteria and 415 anaerobic methanotrophic archaea, with additional aerobic oxidation minimozing 416 atmospheric release (Boetius et al., 2000; Deutzmann and Schink, 2011; Mostovaya et al., 2022). Conversely, thinner oxic layers in lakes permit substantial methane bypass 417 418 of oxidation, leading to significant atmospheric emissions (Sun,2024). 419  $CO_2+4H_2\rightarrow CH_4+2H_2O_1$ (R1) 420  $CH_3COOH \rightarrow CH_4 + CO_2$ (R2)





421 The carbon isotope fractionation between carbonate and organic matter 422  $(\Delta^{13}C = \delta^{13}C_{carb} - \delta^{13}C_{org})$  serves as a valuable proxy for assessing microbial 423 contributions to sedimentary organic carbon. As established in prior studies (Hayes et al., 1999; Teranes and Bernasconi, 2005; Zhu et al., 2013),  $\Delta^{13}$ C approximates  $\epsilon$ TOC, 424 the isotopic fractionation factor during organic matter synthesis. Significantly, &TOC 425 426 value >32% indicates a dominant bacterial contribution to sedimentary organic matter, 427 while values between 28% and 32% suggest a mixed phytoplankton-bacterial source 428 (Hayes et al., 1999; Teranes and Bernasconi, 2005; Zhu et al., 2013). Analysis of the 429 Dingqinghu Formation reveals that intervals characterized by enriched  $\delta C_{carb}$  values predominantly exhibit  $\Delta^{13}$ C values exceeding 32% (Fig. 3). This pronounced 430 431 fractionation strongly implicates bacterial fermentation and decomposition as the 432 primary processes driving carbon isotope dynamics during these stages. Concurrently depleted TOC values align with the expected signature of intense bacterial organic 433 434 matter remineralization, further supporting the inference of methane release associated 435 with these microbial processes. 436 5.3 Lacustrine methane emissions response to Early Miocene warming 437 The Early Miocene was a pivotal period for climatic change in Asia, primarily driven 438 by the extensive uplift of the Tibetan Plateau and the retreat of the Paratethys Ocean. 439 These processes intensified the Asian monsoon system (Ramstein et al., 1997; Liu and 440 Yin, 2002; Zhang et al., 2007; Boos & Kuang, 2010; Clift & Webb, 2019; Spicer et al., 441 2021), altering atmospheric circulation and thermal gradients, which in turn led to 442 significant climatic differentiation across the Tibetan Plateau and adjacent areas. The 443 plateau itself is influenced by both the Indian monsoon and continental monsoon 444 systems, resulting in a range of climate regimes from warm and humid to dry and cold 445 (Kutzbach et al., 1993; Guo et al., 2008; Shukla et al., 2014). 446 Studies by Deng et al. (2019) indicate that during the Miocene, the Indian monsoon 447 dominated the Lunpola Basin, supplying ample moisture and warmth to the region. This 448 interpretation is supported by the presence of subtropical fish fossils in the stratigraphic





record, along with previously documented mammalian fossils, pollen, and spores (Deng et al., 2012; Sun et al., 2014; Jia et al., 2015; Jiang et al., 2018). The monsoon-driven warm and humid conditions fostered high productivity of organic matter within the lake ecosystem, while also promoting the decomposition of organic material by methanogens, leading to substantial methane production (Deng et al., 2019; Su et al., 2019).

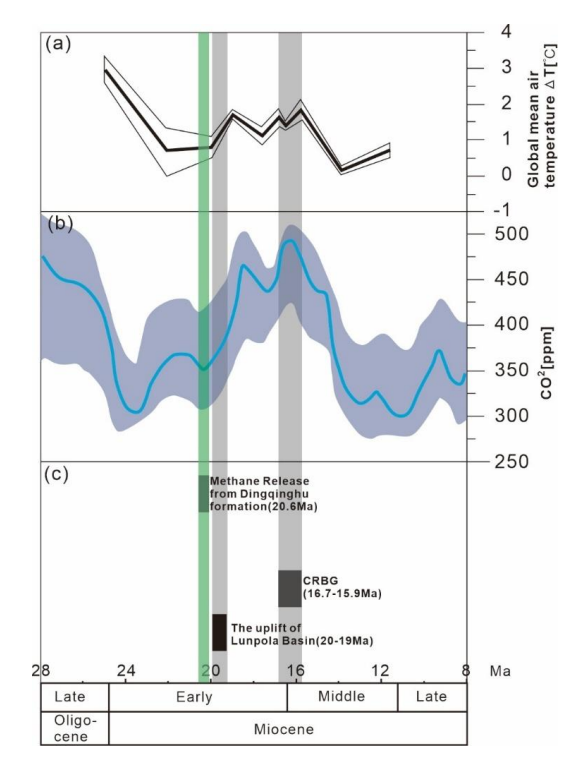


Figure 6:(a)The difference between the global average temperature and today's temperature simulation(Kürschner et al.,2008); (b) Atmospheric CO2 estimates (symbols) and 500-kyr mean statistical reconstructions (95% credible intervals in dark-blue shading, respectively) (Cenozoic CO2 Proxy Integration Project (CenCO<sub>2</sub>PIP) Consortium,2023); (c) Main geological events of the Miocene, From right to left in order: 1) Methane release from Dingqinghu formation (this study) 2) The uplift of Lunpola basin (Li et al.,2024) 3) CRBG: Columbia River Basalt Group, the largest terrestrial volcanic event in North America(Kasbohm et al.,2018).

Geochemical records from the Dingqinghu Formation in the Lunpola Basin reveal





464 severely deficient sulfur content (as indicated by whole-rock S data; see Table S2) along 465 with exceptionally low pyrite abundance, suggesting that sulfate concentrations in the 466 paleo-lake were minimal during deposition. This sulfate-limited environment likely 467 suppressed sulfate-driven anaerobic oxidation of methane (SD-AOM). In addition, a 468 reduced oxidation zone further decreased CH4 consumption, resulting in significant 469 methane efflux into the atmosphere (Fig. 5; Taylor and Macquaker, 2011; Rickard, 2021; 470 Lin et al., 2023). 471 As a potent greenhouse gas, with a global warming potential 28–34 times that of CO<sub>2</sub> 472 over a 100-year period, methane release from lakes could have contributed substantially 473 to global warming (Forster et al., 2008; Sun et al., 2020). The only known Large 474 Igneous Province (LIP) eruption during the Miocene was the Columbia River Basalt Group, which occurred between approximately 16.7 and 15.9 Ma. This event 475 significantly increased global temperatures and atmospheric CO2 levels (Fig. 6c; 476 477 Kasbohm et al., 2018). However, according to Li et al. (2024), major uplift of the Lunpola Basin occurred between 20 and 19 Ma, after the methane release event 478 479 recorded in the Dingqinghu Formation. This temporal discordance indicates that 480 methane release was not triggered by tectonic uplift (Fig. 6). Furthermore, no 481 contemporary volcanic activity was associated with this methane emission, suggesting 482 that climatic and lacustrine thermal conditions were the primary controls. 483 Global temperature reconstructions for the Early Miocene indicate a warming trend, 484 accompanied by methane release and rising atmospheric CO2 levels, which suggests a 485 methane-driven warming event (Fig. 6; Kürschner et al., 2008). In the absence of large 486 igneous province volcanism, this increase in CO2 can likely attributed to two main processes: (1) the atmospheric oxidation of methane released from the lacustrine 487 488 deposits, such as those of the Dingqinghu Formation identified in the present study, and 489 (2) additional CO<sub>2</sub> emissions from climate feedback mechanisms amplified by the 490 initial greenhouse warming (Fig. 6; Cenozoic CO2 Proxy Integration Project 491 (CenCO<sub>2</sub>PIP) Consortium, 2023). Consequently, methane release from the Tibetan





- 492 Plateau may have played an important role in Early Miocene global warming and the
- 493 concurrent rise in atmospheric CO<sub>2</sub> levels.
- 494 As discussed in the preceding sections, a positive feedback mechanism exists
- 495 between methane release in the Dingqinghu Formation and global climate warming
- 496 during the Miocene. As temperature rose, lake stratification and anoxia intensified,
- 497 stimulating microbial methanogenesis and methane ebullition. This released methane
- 498 was subsequently oxidized to CO<sub>2</sub>, further amplifying the greenhouse effect and
- 499 reinforcing the warming cycle. The Dingqinghu Formation represents a deep-water,
- 500 anoxic, organic-rich, and semi-restricted lacustrine system with limited external DIC
- 501 input. To quantify methane ebullition during intervals of pronounced positive carbon
- 502 isotope excursions in lacustrine sediments, we applied a closed-system Rayleigh
- 503 fractionation model (Eq. (2)). This method enables estimation of methane emission
- 504 rates and evaluation of their contribution to atmospheric CO<sub>2</sub>, offering direct numerical
- support for the proposed positive feedback mechanism.
- The Rayleigh distillation equation is expressed as (Höhener and Atteia, 2014; Miller
- 507 et al.,2018; Li et al, 2024):

$$\delta^{13}C_{carb} = \delta^{13}C_{initial} + \varepsilon \cdot ln(f), \tag{2}$$

- where  $\delta^{13}C_{carb}$  is the measured carbonate carbon isotope composition (% VPDB),
- $\delta^{13}$ C<sub>initial</sub> is the initial dissolved inorganic carbon isotope composition (+2%, typical
- 511 lacustrine background) (Lengs and Marshall, 2004);  $\varepsilon$  is the fractionation factor (-20%)
- 512 for acetoclastic methanogenesis) (Penning et al., 2006; Valentine et al., 2004; Meister et
- al.,2019); and f is the fraction of residual DIC.
- The fraction of methane lost from the system is then:

$$1 - f = 1 - exp\left(\frac{\delta^{13}C_{carb} + 2}{-20}\right),\tag{3}$$

Methane ebullition flux (g CH<sub>4</sub> m<sup>-2</sup> kyr<sup>-1</sup>) is calculated as:

517 
$$F_{CH_4} = (1 - f) \times OCBR \times \frac{16}{12},$$
 (4)

- where OCBR is the measured organic carbon burial rate (g C cm<sup>-2</sup> kyr<sup>-1</sup>). Fluxes are
- 519 converted to g CH<sub>4</sub> m<sup>-2</sup> yr<sup>-1</sup> by division by 1000. The full 62-sample dataset with CH4





520 flux is provided in Supplementary Table S4. 521 Our calculations show that the paleo-Dingqinghu Lake maintained an average methane flux of 34.5 g CH<sub>4</sub> m<sup>-2</sup> yr<sup>-1</sup> (peaking at 151.2 g CH<sub>4</sub> m<sup>-2</sup> yr<sup>-1</sup>). After accounting 522 523 for 30-50% methane loss during atmospheric escape and oxidation, these ebullition 524 events contributed an estimated 3.9-6.6 ppm of atmospheric CO<sub>2</sub> throughout the 525 studied depositional interval. These values provide quantitative evidence that Miocene 526 global warming enhanced lake stratification and anoxia, accelerating organic matter 527 decomposition and methane release. The subsequent oxidation of this methane supplied 528 additional CO2 to the atmosphere, further strengthening greenhouse conditions and 529 closing a powerful feedback loop. Therefore, paleo-Dingqinghu Lake serves as a clear 530 example of how continental lacustrine systems on the Tibetan Plateau acted as 531 significant amplifiers of global warming during past greenhouse climates, even though their role had been previously underestimated. 532 533 **Conclusions** 534 Our finds establish that the pronounced positive carbonate carbon isotope excursion 535 (δ<sup>13</sup>C<sub>carb</sub> up to +13.79‰) recorded in the Dingqinghu Formation, Lunpola Basin, 536 originated primarily from large-scale methanogenesis and subsequent methane release. 537 Favorable paleoclimate and tectonic conditions promoted organic matter accumulation and methanogenesis, while low sulfate concentrations limited anaerobic methane 538 539 oxidation, facilitating substantial methane escape to the atmosphere. The observed 540 coupling between this methane release and Early Miocene global atmospheric pCO<sub>2</sub> and temperature rises implicates that Tibetan Plateau methane emissions as a potentially 541 542 important contributor to in Early Miocene global warming and the coeval increase in 543 atmospheric CO<sub>2</sub>. 544 Data availability

# 23

All raw data can be provided by the corresponding authors upon request.





546	Author contributions
547	CY, XF, and HW: study design, data production, analysis, data interpretation, writing.
548	CY, JD, YW, and TW: sample handling. CY: stable isotope and organic carbon content
549	experiment. CY, XF, and SZ: calculation of methane flux.
550	Competing interests
551	The contact author has declared that none of the authors has any competing interests.
552	Acknowledgements
553	We thank Ahmed Mansour for providing comprehensive and valuable suggestions.
554	Financial support
555	This research was supported funding from the National Natural Science Foundation of
556	China (grant numbers 42241203,42241202, w2433105) and Science and Technology
557	Cooperation Project of the CNPC-SWPU Innovation Alliance (2020Cx0101).
558	Reference
559	Altabet, M. A.: Variations in nitrogen isotopic composition between sinking and
560	suspended particles: Implications for nitrogen cycling and particle transforma
561	tion in the open ocean, Deep-Sea Res. Part I-Oceanogr. Res. Pap., 35: 535-5
562	54, https://doi.org/10.1016/0198-0149(88)90130-6, 1988.
563	Altabet, M. A.: Isotopic tracers of the marine nitrogen cycle: present and past,i
564	n: Marine organic matter: biomarkers, isotopes and DNA, edited by: Volkma
565	n, J.K., Springer, Berlin, Heidelberg, 251-293, https://doi.org/10.1007/698_2_0
566	<u>08</u> , 2006
567	Bastviken, D., Cole, J., Pace, M., and Tranvik, L.: Methane emissions from lak
568	es: Dependence of lake characteristics, two regional assessments, and a globa





569 1 estimate, Glob. Biogeochem. Cycle., 18, GB4009, https://doi.org/10.1029/200 570 4GB002238, 2004. Boetius, A., Ravenschlag, K., Schubert, C. J., Rickert, D., Widdel, F., Gieseke, 571 572 A., Amann, R., Jørgensen, B. B., Witte, U., and Pfannkuche, O.: A marine microbial consortium apparently mediating anaerobic oxidation of methane, N 573 ature, 407, 623-626, https://doi.org/10.1038/35036572, 2000. 574 Boos, W. R. and Kuang, Z.: Dominant control of the South Asian monsoon by 575 orographic insulation versus plateau heating, Nature, 463: 218-222, https://do 576 577 i.org/10.1038/nature08707, 2010. Boscolo-Galazzo, F., Crichton, K. A., Ridgwell, A., Mawbey, E. M., Wade, B. 578 579 S., and Pearson, P. N.: Temperature controls carbon cycling and biological e 580 volution in the ocean twilight zone. Science, 371, 1148-1152, https://doi.org/1 581 0.1126/science.abb6643, 2021. Cadeau, P., Jézéquel, D., Leboulanger, C., Fouilland, E., Le Floc'h, E., Chadute 582 583 au, C., Milesi, V., Guélard, J., Sarazin, G., Katz, A., d'Amore, S., Bernard, 584 C., and Ader, M.: Carbon isotope evidence for large methane emissions to t he proterozoic atmosphere, Sci Rep., 10, 18186, https://doi.org/10.1038/s41598 585 -020-75100-x, 2020. 586 587 Calvert, S. E.: Oceanographic controls on the accumulation of organic matter i 588 n marine sediments, Geol. Soc. London. Spec. Publ., 26, 137-151, https://doi. 589 org/10.1144/GSL.SP.1987.026.01.08, 1987.







- 590 Cartapanis, O., Bianchi, D., Jaccard, S. L., and Galbraith, E. D.: Global pulses
- of organic carbon burial in deep-sea sediments during glacial maxima, Nat.
- 592 Commun., 7, 10796, <a href="https://doi.org/10.1038/ncomms10796">https://doi.org/10.1038/ncomms10796</a>, 2016.
- 593 Cenozoic CO<sub>2</sub> Proxy Integration Project (CenCO<sub>2</sub>PIP) Consortium: Toward a C
- enozoic history of atmospheric CO<sub>2</sub>, Science, 382, eadi5177, https://doi.org/1
- 595 <u>0.1126/science.adi5177</u>, 2023.
- 596 Clift, P. D. and Webb, A. A. G.: A history of the Asian monsoon and its inte
- 597 ractions with solid Earth tectonics in Cenozoic South Asia, Geol. Soc. Spec.
- 598 Publ., 483, 631-652, https://doi.org/10.1144/SP483.1, 2019.
- 599 De Boever, E., Brasier, A. T., Foubert, A., and Kele, S.: What do we really k
- 600 now about early diagenesis of non-marine carbonates? Sediment. Geol., 361,
- 601 25–51, <a href="https://doi.org/10.1016/j.sedgeo.2017.09.011">https://doi.org/10.1016/j.sedgeo.2017.09.011</a>, 2017.
- Dean, J. F., Middelburg, J. J., Röckmann, T., Aerts, R., Blauw, L. G., Egger,
- 603 M., Jetten, M. S. M., de Jong, A. E. E., Meisel, O. H., Rasigraf, O., Slomp,
- 604 C. P., In'T Zandt, M. H., and Dolman, A. J.: Methane feedbacks to the glo
- bal climate system in a warmer world, Rev. Geophys., 56, 207-250, https://d
- 606 <u>oi.org/10.1002/2017RG000559</u>, 2018.
- 607 DelSontro, T., Boutet, L., St-Pierre, A., Del Giorgio, P. A., and Prairie, Y. T.:
- Methane ebullition and diffusion from northern ponds and lakes regulated by
- the interaction between temperature and system productivity, Limnol. Oceano
- 610 gr., 61: S62-S77, https://doi.org/10.1002/lno.10335, 2016.





611 Deng, T., Wang, S., Xie, G., Li, Q., Hou, S., and Sun, B.: A mammalian fossi 612 1 from the Dingqing Formation in the Lunpola Basin, northern Tibet, and its 613 relevance to age and paleo-altimetry, Chin. Sci. Bull., 57, 261-269, https://do 614 i.org/10.1007/s11434-011-4773-8, 2012. 615 Deng, T., Wang, X., Wu, F., Wang, Y., Li, Q., Wang, S., and Hou, S.: Implica 616 tions of vertebrate fossils for paleo-elevations of the Tibetan Plateau, Glob. 617 Planet. Change, 174, 58-69, https://doi.org/10.1016/j.gloplacha.2019.01.005, 20 618 19. 619 Deutzmann, J. S., and Schink, B.: Anaerobic oxidation of methane in sediment 620 s of Lake Constance, an oligotrophic freshwater lake, Appl. Environ. Microbi 621 ol., 77, 4429-4436, <a href="https://doi.org/10.1128/AEM.00340-11">https://doi.org/10.1128/AEM.00340-11</a>, 2011. 622 Encinas Fernández, J., Peeters, F., and Hofmann, H.: Importance of the autumn 623 overturn and anoxic conditions in the hypolimnion for the annual methane 624 625 //doi.org/10.1021/es4056164, 2014. 626 Fang, X., Dupont-Nivet, G., Wang, C., Song, C., Meng, Q., Zhang, W., Nie, J., 627 Zhang, T., Mao, Z., and Chen, Y.: Revised chronology of central Tibet upli 628 ft (Lunpola Basin), Sci. Adv., 6, eaba7298, http://doi.org/10.1126/sciadv.aba72 629 <u>98</u>, 2020. Forster, P., Ramaswamy, V., Artaxo, P., Berntsen, T., Betts, R., Fahey, D., Hay 630 631 wood, J., Lean, J., Lowe, D., Myhre, G., Nganga, J., Prinn, R., Raga, G., S





632 chulz, M., and Van Dorland, R.: Changes in atmospheric constituents and in radiative forcing, in: Climate Change 2007: The Physical Science Basis, edite 633 634 d by: Solomon, S., Qin, D., Manning, M., Marquis, M., Averyet, K., and M 635 elinda M. B., Cambridge University Press, Cambridge, UK, 129-134, ISBN 9780521705967, 2008. 636 637 Freudenthal, T., Wagner, T., Wenzhöfer, F., Zabel, M., and Wefer, G.: Early dia genesis of organic matter from sediments of the eastern subtropical Atlantic: 638 evidence from stable nitrogen and carbon isotopes, Geochim. Cosmochim. Ac 639 640 ta, 65, 1795-1808, https://doi.org/10.1016/S0016-7037(01)00554-3, 2001. 641 Fu, X., Wang, J., Tan, F., Feng, X., Wang, D., and Song, C.: Geochemistry of 642 terrestrial oil shale from the Lunpola area, northern Tibet, China, Int. J. Coal 643 Geol., 102, 1-11, https://doi.org/10.1016/j.coal.2012.08.005, 2012. Fu, X., Wang, J., Chen, W., Feng, X., Wang, D., Song, C., and Zeng, S.: Org 644 645 anic accumulation in lacustrine rift basin: constraints from mineralogical and 646 multiple geochemical proxies, Int. J. Earth Sci., 104, 495-511, https://doi.org/ 647 10.1007/s00531-014-1089-3, 2015. 648 Fu, X., Wang, J., Wen, H., Wang, Z., Zeng, S., Song, C., Wang, D., and Nie, 649 Y.: Carbon-isotope record and paleoceanographic changes prior to the OAE 650 1a in the Eastern Tethys: Implication for the accumulation of organic-rich se 651 diments, Mar. Pet. Geol., 113, 104049, https://doi.org/10.1016/j.marpetgeo.201 652 <u>9.104049</u>, 2020.





653 Gravina, P., Ludovisi, A., Moroni, B., Vivani, R., Selvaggi, R., Petroselli, C., a 654 nd Cappelletti, D.: Geochemical proxies and mineralogical fingerprints of sed 655 imentary processes in a closed shallow lake basin since 1850, Aquat. Geoche 656 m., 28, 43-62, https://doi.org/10.1007/s10498-022-09403-y, 2022. Gu, B., Schelske, C. L., and Hodell, D. A.: Extreme 13c enrichments in a sha 657 658 llow hypereutrophic lake: implications for carbon cycling, Limnol. Oceanogr., 659 49, 1152-1159, https://doi.org/10.4319/lo.2004.49.4.1152, 2004. Guo, Z., Sun, B., Zhang, Z., Peng, S., Xiao, G., Ge, J., Hao, Q., Qiao, Y., Li 660 ang, M., Liu, J., Yin, Q., and Wei, J.: A major reorganization of Asian clim 661 662 ate by the early Miocene, Clim. Past, 4, 153-174, https://doi.org/10.5194/cp-4 663 <u>-153-2008</u>, 2008. 664 Gutjahr, M., Ridgwell, A., Sexton, P. F., Anagnostou, E., Pearson, P. N., Pälik 665 e, H., Norris, R. D., Thomas, E., and Foster, G. L.: Very large release of m 666 ostly volcanic carbon during the Palaeocene-Eocene Thermal Maximum, Natu 667 re, 548, 573-577, https://doi.org/10.1038/nature23646, 2017. 668 Han, L., Li, Y., Zou, Y., Gao, X., Gu, Y., and Wang, L.: Relationship between 669 lake salinity and the climatic gradient in northeastern China and its implicat 670 ions for studying climate change, Sci. Total Environ., 805: 150403, https://do 671 i.org/10.1016/j.scitotenv.2021.150403, 2022. 672 Hayes, J. M., Strauss, H., and Kaufman, A. J.: The abundance of 13C in mari 673 ne organic matter and isotopic fractionation in the global biogeochemical cyc





674 le of carbonduring the past 800 Ma, Chem. Geol., 161, 103-125, https://doi.o 675 rg/10.1016/S0009-2541(99)00083-2, 1999. 676 Hillaire-Marcel, C., Kim, S., Landais, A., Ghosh, P., Assonov, S., Lécuyer, C., 677 Blanchard, M., Meijer, H. A. J., and Steen-Larsen, H. C.: A stable isotope t oolbox for water and inorganic carbon cycle studies, Nat. Rev. Earth. Env., 678 2, 699-719, http://doi.org/10.1038/s43017-021-00209-0, 2021. 679 680 Hodell, D. A. and Schelske, C. L.: Production, sedimentation, and isotopic com 681 position of organic matter in Lake Ontario, Limnol. Oceanogr., 43, 200-214, 682 https://doi.org/10.4319/lo.1998.43.2.0200, 1998. 683 Höhener, P. and Atteia, O.: Rayleigh equation for evolution of stable isotope ra 684 tios in contaminant decay chains, Geochim. Cosmochim. Acta, 126, 70-77, ht 685 tps://doi.org/10.1016/j.gca.2013.10.036, 2013. Hollander, D. J. and Smith, M. A.: Microbially mediated carbon cycling as a c 686 ontrol on the  $\delta^{13}$ C of sedimentary carbon in eutrophic Lake Mendota (USA): 687 688 new models for interpreting isotopic excursions in the sedimentary record, 689 Geochim. Cosmochim. Acta, 65, 4321-4337, https://doi.org/10.1016/S0016-703 690 <u>7(00)00506-8</u>, 2001. 691 Horacek M., Brandner R., and Abart R.: Carbon isotope record of the P/T bou 692 ndary and the Lower Triassic in the Southern Alps: evidence for rapid chan ges in storage of organic carbon, Paleogeogr. Paleoclimatol. Paleoecol., 252, 693 694 347-354, https://doi.org/10.1016/j.palaeo.2006.11.049, 2007.





- 695 Hu, D., Li, D., Zhou, L., Sun, L., and Xu, Y.: Diagenetic effects on strontium
- 696 isotope (87 Sr/86 Sr) and elemental (Sr, Mn, and Fe) signatures of Late Ordo
- vician carbonates, J. Univ. Sci. Technol. China, 53, 0503-1-0503-10, http://do
- 698 <u>i.org/10.52396/JUSTC-2022-0160</u>, 2023.
- 699 Huntington K. W. and Petersen S. V.: Frontiers of carbonate clumped isotope t
- hermometry, Annu. Rev. Earth Planet. Sci., 51, 611-641, https://doi.org/10.114
- 701 <u>6/annurev-earth-031621-085949</u>, 2023.
- 702 Ingall, E. D., and Cappellen, P. V.: Relation between sedimentation rate and bu
- 703 rial of organic phosphorus and organic carbon in marine sediments, Geochim.
- 704 Cosmochim. Acta, 54, 373–386, https://doi.org/10.1016/0016-7037(90)90326-
- 705 <u>G</u>, 1990.
- 706 Ivany, L. C., del Río, C. J., Alvarez, M. J., Acosta, R. P., Lohmann, K. C., a
- 707 nd Raigemborn, M. S.: Approaching the Miocene Climatic Optimum in Pata
- 708 gonia (southern Argentina): Temperature seasonality and a potential role for t
- he opening Drake Passage, Paleoceanogr. Paleoclimatology, 40, e2025PA0051
- 710 00, <a href="https://doi.org/10.1029/2025PA005100">https://doi.org/10.1029/2025PA005100</a>, 2025.
- 711 Kender, S., Bogus, K., Pedersen, G. K., Dybkjær, K., Mather, T. A., Mariani,
- 712 E., Ridgwell, A., Riding, J. B., Wagner, T., Hesselbo, S. P., and Leng, M. J.:
- 713 Paleocene/Eocene carbon feedbacks triggered by volcanic activity, Nat. Com
- 714 mun., 12, 5186, https://doi.org/10.1038/s41467-021-25536-0, 2021.
- 715 Kipp, M. A., Stüeken, E. E., Yun, M., Bekker, A., and Buick, R.: Pervasive a





716 ero-bic nitrogen cycling in the surface ocean across the Paleopro-terozoic Er 717 a, Earth Planet. Sci. Lett., 500,117-126, https://doi.org/10.1016/j.epsl.2018.08.0 718 <u>07</u>, 2018. 719 Kürschner, W. M., Kvaček, Z., and Dilcher, D. L.: The impact of Miocene at 720 mospheric carbon dioxide fluctuations on climate and the evolution of terrest rial ecosystems, Proc. Natl. Acad. Sci., 105, 449-453, http://doi.org/10.1073/p 721 722 nas.0708588105, 2008. 723 Lamb, H. F., Leng, M. J., Telford, R. J., Ayenew, T., and Umer, M.: Oxygen 724 and carbon isotope composition of authigenic carbonate from an Ethiopian la 725 ke: a climate record of the last 2000 years, The Holocene, 17, 515-524, http: 726 //doi.org/10.1177/0959683607076452, 2007. 727 Lehmann, M. F., Bernasconi, S. M., Barbieri, A., and Mckenzie, J. A.: Preserv 728 ation of organic matter and alteration of its carbon and nitrogen isotope com 729 position during simulated and in situ early sedimentary diagenesis, Geochim. 730 Cosmochim. Acta, 2002, 3573-3584, https://doi.org/10.1016/S0016-7037(02)009 731 68-7, 2002. 732 Lei Q., Fu X., and Lu Y.: Petroleum geological features of Tertiary terrestrial 733 Lunpola basin, Tibet,in: Geology of Fossil Fuels --- Oil and Gas: Proceedin 734 gs of the 30th International Geological Congress, edited by: Sun, Z.C., Wan g, T.B., Ye, D.L., and Song, G.J., 11, https://doi.org/10.1201/9780429087837, 735 736 1997.





- 737 Leng, M. J. and Marshall, J. D.: Palaeoclimate interpretation of stable isotope
- data from lake sediment archives, Quat. Sci. Rev., 23, 811-831, https://doi.or
- 739 <u>g/10.1016/j.quascirev.2003.06.012</u>, 2004.
- 740 Li, L., Garzione, C. N., Lu, H., and Quade, J.: Neogene surface uplift of the
- 741 Lunpola Basin in Central Tibet: Implications for uplifting and flattening of o
- rogenic plateaus, Earth Planet. Sci. Lett., 646, 118961, https://doi.org/10.1016/
- 743 <u>j.epsl.2024.118961</u>, 2024.
- 744 Li, W., Wang, J., Jia, C., Lu, S., Li, J., Zhang, P., Wei, Y., Song, Z., Chen,
- 745 G., and Zhou, N.: Carbon isotope fractionation during methane transport thro
- 746 ugh tight sedimentary rocks: phenomena, mechanisms, characterization, and i
- 747 mplications, Geosci. Front., 15, 101912, <a href="https://doi.org/10.1016/j.gsf.2024.1019">https://doi.org/10.1016/j.gsf.2024.1019</a>
- 748 <u>12</u>, 2024.
- 749 Lin, Z., Strauss, H., Peckmann, J., Roberts, A. P., Lu, Y., Sun, X., Chen, T., a
- 750 nd Harzhauser, M.: Seawater sulphate heritage governed early late miocene
- 751 methane consumption in the long-lived lake pannon, Commun. Earth Enviro
- 752 n., 4, 207, https://doi.org/10.1038/s43247-023-00879-2, 2023.
- 753 Liu, X. and Yin, Z.: Sensitivity of East asian monsoon climate to the uplift of
- 754 the Tibetan Plateau, Palaeogeogr, Palaeoclimatol. Palaeoecol., 183, 223–245,
- 755 <u>https://doi.org/10.1016/S0031-0182(01)00488-6</u>, 2002.
- 756 Liu, Q., Li, P., Jin, Z., Sun, Y., Hu, G., Zhu, D., Huang, Z., Liang, X., Zhan
- 757 g, R., and Liu, J.: Organic-rich formation and hydrocarbon enrichment of lac





- ustrine shale strata: A case study of Chang 7 Member, Sci. China Earth Sci.,
- 759 65, 118-138, <a href="https://doi.org/10.1007/s11430-021-9819-y">https://doi.org/10.1007/s11430-021-9819-y</a>, 2022.
- 760 Lourey, M. J., Trull, T. W., and Sigman, D. M.: Sensitivity of δ15N of nitrate,
- surface suspended and deep sinking particulate nitrogen to seasonal nitrate d
- epletion in the Southern Ocean, Glob. Biogeochem. Cycle., 17, 1081, https://
- 763 <u>doi.org/10.1029/2002GB001973</u>, 2003.
- 764 Lu, Y., Meyers, P. A., Eadie, B. J., and Robbins, J. A.: Carbon cycling in Lak
- 765 e Erie during cultural eutrophication over the last century inferred from the
- stable carbon isotope composition of sediments, J. Paleolimn., 43, 261-272, h
- 767 <u>ttps://doi.org/10.1007/s10933-009-9330-y</u>, 2010.
- 768 Lu, J., Fu, X., Du, Q., Nie, Y., Wei, H., Zhou, G., and Wang, W.: Climate-ind
- 769 uced organic matter enrichment in lacustrine basin: Insights from the Palaeog
- ene-Neogene oil shale in the Lunpola Basin (Tibet, China), Geol. J., 2023,
- 58, 4057-4069, <a href="https://doi.org/10.1002/gj.4758">https://doi.org/10.1002/gj.4758</a>, 2023.
- 772 Bižić, M., Klintzsch, T., Ionescu, D., Hindiyeh, M. Y., Günthel, M., Muro-Past
- or, A. M., Eckert, W., Urich, T., Keppler, F., and Grossart, H. P.: Aquatic a
- 774 nd terrestrial cyanobacteria produce methane, Sci. Adv., 6, eaax5343, http://d
- 775 <u>x.doi.org/10.1126/sciadv.aax5343</u>, 2020.
- 776 Ma, P., Wang, L., Wang, C., Wu, X., and Wei, Y.: Organic-matter accumulatio
- 777 n of the lacustrine Lunpola oil shale, central Tibetan Plateau: Controlled by
- the paleoclimate, provenance, and drainage system, Int. J. Coal Geol., 147-1





- 779 48, 58–70, <a href="https://doi.org/10.1016/j.coal.2015.06.011">https://doi.org/10.1016/j.coal.2015.06.011</a>, 2015.
- 780 Ma, P., Wang, C., Meng, J., Ma, C., Zhao, X., Li, Y., and Wang, M.: Late Ol
- 781 igocene-early Miocene evolution of the Lunpola Basin, central Tibetan Platea
- 782 u, evidences from successive lacustrine records, Gondwana Res., 48: 224-236,
- 783 <u>https://doi.org/10.1016/j.gr.2017.04.023</u>, 2017.
- 784 Macko, S. A., Fogel, M. L., Hare, P. E., and Hoering, T. C.: Isotopic fractiona
- 785 tion of nitrogen and carbon in the synthesis of amino acids by microorganis
- 786 ms, Chemical Geology: Isotope Geoscience section, 65, 79-92, https://doi.org/
- 787 10.1016/0168-9622(87)90064-9, 1987.
- 788 Mao, Z., Meng, Q., Fang, X., Zhang, T., Wu, F., Yang, Y., Zhang, W., Zan, J.,
- and Tan, M.: Recognition of tuffs in the middle-upper dingqinghu fm., Lun
- 790 pola basin, central tibetan plateau: constraints on stratigraphic age and implic
- 791 ations for paleoclimate, Paleogeogr. Paleoclimatol. Paleoecol., 525, 44-56, htt
- 792 ps://doi.org/10.1016/j.palaeo.2019.03.040, 2019.
- 793 Martens C. S. and Berner R. A.: Methane production in the interstitial waters
- of sulfate-depleted marine sediments, Science, 185, 1167-1169, <a href="http://dx.doi.or">http://dx.doi.or</a>
- 795 <u>g/10.1126/science.185.4157.1167</u>, 1974.
- 796 McCormack, J., Viehberg, F., Akdemir, D., Immenhauser, A., and Kwiecien, O.:
- 797 Ostracods as ecological and isotopic indicators of lake water salinity change
- s: the Lake Van example, Biogeosciences, 16, 2095-2114, https://doi.org/10.51
- 799 <u>94/bg-16-2095-2019</u>, 2019.





800 Meister, P., Liu, B., Khalili, A., Böttcher, M.E., and Jørgensen, B.B.: Factors c 801 ontrolling the carbon isotope composition of dissolved inorganic carbon and 802 methane in marine porewater: an evaluation by reaction-transport modelling, J. Mar. Syst., 200, 103227, https://doi.org/10.1016/j.jmarsys.2019.103227, 201 803 804 9. 805 Methner, K., Campani, M., Fiebig, J., Löffler, N., Kempf, O., and Mulch, A.: 806 Middle Miocene long-term continental temperature change in and out of pace 807 with marine climate records, Sci Rep, 10, 7989, https://doi.org/10.1038/s415 808 98-020-64743-5, 2020. 809 Mettam, C., Zerkle, A. L., Claire, M. W., Prave, A. R., Poulton, S. W., and J 810 unium, C. K.: Anaero-bic nitrogen cycling on a Neoarchaean ocean margin, 811 Earth Planet. Sci. Lett., 527, 115800, https://doi.org/10.1016/j.epsl.2019.11580 812 <u>0</u>, 2019. 813 Meyers, P. A.: Organic geochemical proxies of paleoceanographic, paleolimnolo 814 gic, and paleoclimatic processes, Org. Geochem., 27, 213-250, https://doi.org/ 815 10.1016/S0146-6380(97)00049-1, 1997. 816 Michener, R., and Lajtha, K. (Eds.): Stable isotopes in ecology and environmen 817 tal science, John Wiley and Sons, 566pp., ISBN 9780470691854, 2008. 818 Miller, H.M., Chaudhry, N., Conrad, M.E., Bill, M., Kopf, S.H., and Templeto 819 n, A.S.: Large carbon isotope variability during methanogenesis under alkalin 820 e conditions, Geochim. Cosmochim. Acta, 237, 18-31, https://doi.org/10.1016/





821 j.gca.2018.06.007, 2018. 822 Mor, Z., Assouline, S., Tanny, J., Lensky, I. M., and Lensky, N. G.: Effect of 823 water surface salinity on evaporation: The case of a diluted buoyant plume o ver the Dead Sea, Water Resour. Res., 54, 1460-1475, https://doi.org/10.1002/ 824 825 2017WR021995, 2018. 826 Mostovaya, A., Wind-Hansen, M., Rousteau, P., Bristow, L. A., and Thamdrup, 827 B.: Sulfate-and iron-dependent anaerobic methane oxidation occurring side-by-828 side in freshwater lake sediment, Limnol. Oceanogr., 67, 231-246, https://doi. 829 org/10.1002/lno.11988, 2022. 830 Müller, P. J. and Suess, E.: Productivity, sedimentation rate, and sedimentary or 831 ganic matter in the oceans-I. Organic carbon preservation. Deep-Sea Res. Pa 832 rt I-Oceanogr. Res. Pap., 26, 1347-1362, https://doi.org/10.1016/0198-0149(79) 833 90003-7, 1979. 834 Neumann, T., Stögbauer, A., Walpersdorf, E., Stüben, D., and Kunzendorf, H.: 835 Stable isotopes in recent sediments of Lake Arendsee, NE Germany: respons 836 e to eutrophication and remediation measures, Paleogeogr. Paleoclimatol. Pale 837 oecol., 178, 75-90, https://doi.org/10.1016/S0031-0182(01)00403-5, 2002. 838 Nie, Y., Fu, X., Liu, X., Wei, H., Zeng, S., Lin, F., Wan, Y., and Song, C.: O 839 rganic matter accumulation mechanism under global/regional warming: Insight 840 from the Late Barremian calcareous shales in the Qiangtang Basin (Tibet), 841 J. Asian Earth Sci., 241: 105456, https://doi.org/10.1016/j.jseaes.2022.105456,





842 2023. Papineau, D., Purohit, R., Goldberg, T., Pi, D., Shields, G. A., Bhu, H., Steele, 843 844 A., and Fogel, M. L.: High primary productivity and nitrogen cycling after 845 the Paleoproterozoic phosphogenic event in the Aravalli Supergroup, India, Pr 846 ecambrian Res., 171, 37-56, https://doi.org/10.1016/j.precamres.2009.03.005, 20 09. 847 Penning, H., Claus, P., Casper, P., and Conrad, R.: Carbon isotope fractionation 848 849 during acetoclastic methanogenesis by methanosaeta concilii in culture and a 850 lake sediment, Appl. Environ. Microbiol., 72, 5648-5652, https://doi.org/10.1 851 128/AEM.00727-06, 2006. 852 Ramstein, G., Fluteau, F., Besse, J., and Joussaume, S.: Effect of orogeny, plat 853 e motion and land-sea distribution on Eurasian climate change over the past 854 30 million years, Nature, 386, 788-795, https://doi.org/10.1038/386788a0, 199 855 7. 856 Rickard, D. (Eds.): Framboids, Oxford University Press, Oxford Academic, http 857 s://doi.org/10.1093/oso/9780190080112.001.0001,2021. 858 Ritter, A., Mavromatis, V., Dietzel, M., Kwiecien, O., Wiethoff, F., Griesshaber, 859 E., Casella, L. A., Schmahl, W. W., Koelen, J., Neuser, R. D., Leis, A., B 860 uhl, D., Niedermayr, A., Breitenbach, S. F. M., Bernasconi, S. M., and Imm 861 enhauser, A.: Exploring the impact of diagenesis on (isotope) geochemical an 862 d microstructural alteration features in biogenic aragonite, Sedimentology, 64,





- 863 1354-1380, https://doi.org/10.1111/sed.12356, 2017.
- 864 Robinson, R. S., Kienast, M., Luiza Albuquerque, A., Altabet, M., Contreras,
- 865 S., De Pol Holz, R., Dubois, N., Francois, R., Galbraith, E., Hsu, T., Ivanoc
- 866 hko, T., Jaccard, S., Kao, S., Kiefer, T., Kienast, S., Lehmann, M., Martinez,
- P., Mccarthy, M., Möbius, J., Pedersen, T., Quan, T. M., Ryabenko, E., Sch
- 868 mittner, A., Schneider, R., Schneider-Mor, A., Shigemitsu, M., Sinclair, D., S
- 869 omes, C., Studer, A., Thunell, R., and Yang, J.: A review of nitrogen isotopi
- c alteration in marine sediments, Paleoceanography, 2012, 27, PA4203, https://
- 871 /doi.org/10.1029/2012PA002321, 2012.
- 872 Rowley, D. and Currie, B.: Palaeo-altimetry of the late Eocene to Miocene Lu
- npola basin, central Tibet, Nature, 439, 677-681, https://doi.org/10.1038/nature
- 874 <u>04506</u>, 2006.
- 875 Schelske, C. L. and Hodell, D. A.: Recent changes in productivity and climate
- of LakeOntario detected by isotopic analysis of sediments, Limnol. Oceanogr.,
- 877 36, 961-975, <a href="https://doi.org/10.4319/lo.1991.36.5.0961">https://doi.org/10.4319/lo.1991.36.5.0961</a>, 1991.
- 878 Shen, R. F., Cai, H., and Gong, W. H.: Transgenic Bt cotton has no apparent
- 879 effect on enzymatic activities or functional diversity of microbial communitie
- 880 s in rhizosphere soil, Plant Soil, 285, 149-159, https://doi.org/10.1007/s11104-
- 881 <u>006-9000-z</u>, 2006.
- 882 Shukla, A., Mehrotra, R. C., Spicer, R. A., Spicer, T. E. V., and Kumar, M.:
- 883 Cool equatorial terrestrial temperatures and the South Asian monsoon in the





884 Early Eocene: Evidence from the Gurha Mine, Rajasthan, India, Paleogeogr. 885 Paleoclimatol. Paleoecol., 412, 187-198, https://doi.org/10.1016/j.palaeo.2014.0 886 <u>8.004</u>, 2014. 887 Sigman, D. M., Karsh, K. L., and Casciotti, K. L.: Ocean Process Tracers: Nit 888 rogen Isotopes in the Ocean, in: Encyclopedia of Ocean Sciences, edited by: Steel, J., Thorpe, S., and Turekian, K., Academic Press,4138-4153, https://hdl. 889 890 handle.net/102.100.100/534313, 2009. 891 Spicer, R. A., Su, T., Valdes, P. J., Farnsworth, A., Wu, F., Shi, G., Spicer, T. 892 E. V., and Zhou, Z.: The topographic evolution of the Tibetan Region as rev 893 ealed by palaeontology, Palaeobiodiversity Palaeoenvironments, 101, 213-243, 894 https://doi.org/10.1007/s12549-020-00452-1, 2021. 895 Su, B., Sun, J., and Jin, C.: Orbital forcing of climatic changes on the central 896 tibetan plateau reveals late oligocene to early miocene south asian monsoon 897 evolution, Geophys. Res. Lett., 49, e2021GL097428, https://doi.org/10.1029/20 898 21GL097428, 2022. 899 Sun, F., Hu, W., Wang, X., Cao, J., Fu, B., Wu, H., and Yang, S.: Methanoge 900 n microfossils and methanogenesis in permian lake deposits, Geology, 49, 13 901 -18, https://doi.org/10.1130/G47857.1, 2020. 902 Sun, F., Hu, W., Cao, J., Wang, X., Zhang, Z., Ramezani, J., and Shen, S.: Su 903 stained and intensified lacustrine methane cycling during Early Permian clima 904 te warming, Nat. Commun., 13, 4856, https://doi.org/10.1038/s41467-022-3243





905 8-2, 2022. Sun, F., Luo, G., Pancost, R. D., Dong, Z., Li, Z., Wang, H., Chen, Z., and 906 907 Xie, S.: Methane fueled lake pelagic food webs in a cretaceous greenhouse world, Proc. Natl. Acad. Sci., 121, e2411413121, https://doi.org/10.1073/pnas. 908 909 2411413121, 2024. 910 Talbot, M. R.: Nitrogen isotopes in palaeolimnology, in: Tracking environmental 911 change using lake sediments: physical and geochemical methods, edited by: 912 Last, W.M. and Smol, J.P., Springer, Dordrecht ,2, 401-439, https://doi.org/10. 913 1007/0-306-47670-3 15, 2002. 914 Taylor, K. G. and Macquaker, J. H. S.: Iron minerals in marine sediments reco 915 rd chemical environments, Elements, 7, 113-118, https://doi.org/10.2113/gsele 916 ments.7.2.113, 2011. 917 Tegler, L. A., Horner, T. J., Galy, V. V., Bent, S., Wang, Y., Kim, H. H., Met 918 e, O. Z., and Nielsen, S. G.: Distribution and drivers of organic carbon sedi 919 mentation along the continental margins, AGU Adv., 5, e2023AV001000, http 920 s://doi.org/10.1029/2023AV001000, 2024. 921 Teranes, J. L., Mckenzie, J. A., Lotter, A. F., and Sturm, M.: Stable isotope re 922 sponse to lake eutrophication: calibration of a high-resolution lacustrine seque 923 nce from Baldeggersee, Switzerland, Limnol. Oceanogr., 44, 320-333, https:// 924 doi.org/10.4319/lo.1999.44.2.0320, 1999. Teranes, J. L. and Bernasconi, S. M.: Factors controlling δ<sup>13</sup>C values of sedim 925





926 entary carbon in hypertrophic Baldeggersee, Switzerland, and implications for 927 interpreting isotope excursions in lake sedimentary records, Limnol. Oceanog r., 50, 914-922, https://doi.org/10.4319/lo.2005.50.3.0914, 2005. 928 Thottathil, S. D., Reis, P. C. J., and Prairie, Y. T.: Variability and controls of 929 930 stable carbon isotopic fractionation during aerobic methane oxidation in temp erate lakes, Front. Environ. Sci., 10, 833688, https://doi.org/10.3389/fenvs.202 931 932 2.833688, 2022. 933 Tremblin, M., Khozyem, H., Adatte, T., Spangenberg, J. E., Fillon, C., Grauls, 934 A., Hunger, T., Nowak, A., Läuchli, C., Lasseur, E., Roig, J., Serrano, O., C alassou, S., Guillocheau, F., and Castelltort, S.: Mercury enrichments of the 935 936 Pyrenean foreland basins sediments support enhanced volcanism during the P 937 aleocene-Eocene thermal maximum (PETM), Glob. Planet. Change, 212, 1037 938 94, https://doi.org/10.1016/j.gloplacha.2022.103794, 2022. 939 Tyson, R. V.: Sedimentation rate, dilution, preservation and total organic carbon: 940 some results of a modelling study, Org. Geochem., 32, 333-339, https://doi. 941 org/10.1016/S0146-6380(00)00161-3, 2001. 942 Valentine, D.L., Chidthaisong, A., Rice, A., Reeburgh, W.S., and Tyler, S.C.: C 943 arbon and hydrogen isotope fractionation by moderately thermophilic methano 944 gens, Geochim. Cosmochim. Acta, 68, 1571-1590, https://doi.org/10.1016/j.gca. 945 2003.10.012, 2004. 946 Wang, C., Zhao, X., Liu, Z., Lippert, P. C., Graham, S. A., Coe, R. S., Yi, H.,





947 Zhu, L., Liu, S., and Li, Y.: Constraints on the early uplift history of the Tibetan Plateau, Proc. Natl. Acad. Sci., 105, 4987-4992, https://doi.org/10.107 948 3/pnas.0703595105, 2008. 949 950 Wang, G., Jia, Y., and Li, W.: Effects of environmental and biotic factors on c 951 arbon isotopic fractionation during decomposition of soil organic matter, Sci 952 Rep, 5, 11043, https://doi.org/10.1038/srep11043, 2015. 953 Wang, D., Liu, Y., Zhang, J., Lang, Y., Li, Z., Tong, Z., Xu, L., Su, Z., and 954 Niu, J.: Controls on marine primary productivity variation and organic matter 955 accumulationduring the Late Ordovician-Early Silurian transition, Mar. Pet. 956 Geol., 142, 105742, https://doi.org/10.1016/j.marpetgeo.2022.105742, 2022. Wang, J., Wang, Z., Fu, X., Wang, X., Wilde, S.A., Fu, Y., Lin, J., Wei, H., 957 958 Shen, L., Rao, G., and Mansour, A.: Control of stepwise subduction and sla 959 b breakoff on volcanism and uplift in the Tibetan Plateau, Earth Planet. Sci. Lett., 647, 119057, https://doi.org/10.1016/j.epsl.2024.119057, 2024. 960 961 Wang, L., Li, Y., Shen, L., Han, Z., Peng, H., Li, X., and Wei, Y.: Sedimentar 962 y evolution and hydrocarbon resource potential of Cenozoic continental basin 963 s in the Tibetan Plateau, Acta Petrol. Sin., 41, 1101-1119, https://doi.org/10.1 964 <u>8654/1000-0569/2025.03.20</u>, 2025. 965 Wei, W., Lu, Y., Xing, F., Liu, Z., Pan, L., and Algeo, T. J.: Sedimentary faci 966 es associations and sequence stratigraphy of source and reservoir rocks of th 967 e lacustrine Eocene Niubao Formation (Lunpola Basin, central Tibet), Mar. P





- 968 et. Geol., 86, 1273–1290, https://doi.org/10.1016/j.marpetgeo.2017.07.032, 201
- 969 7.
- 970 Whiticar, M. J.: Carbon and hydrogen isotope systematics of bacterial formatio
- n and oxidation of methane, Chem. Geol., 161, 291-314, https://doi.org/10.10
- 972 <u>16/S0009-2541(99)00092-3</u>, 1999.
- 973 Wynn, J. G.: Carbon isotope fractionation during decomposition of organic matt
- 974 er in soils and paleosols: Implications for paleoecological interpretations of p
- 975 aleosols, Paleogeogr. Paleoclimatol. Paleoecol., 251, 437-448, https://doi.org/1
- 976 0.1016/j.palaeo.2007.04.009, 2007.
- 977 Xia, L., Cao, J., Stüeken, E. E., Hu, W., and Zhi, D.: Linkages between nitrog
- 978 en cycling, nitrogen isotopes, and environmental properties in paleo-lake basi
- 979 ns, Geol. Soc. Am. Bull., 134, 2359-2372, https://doi.org/10.1130/B36290.1, 2
- 980 022.
- 981 Xie, Y., Balázs, A., Gerya, T., and Xiong, X.: Uplift of the Tibetan Plateau dr
- 982 iven by mantle delamination from the overriding plate, Nat. Geosci., 17, 683
- 983 -688, <a href="https://doi.org/10.1038/s41561-024-01473-7">https://doi.org/10.1038/s41561-024-01473-7</a>, 2024.
- 984 Xie, G., Li, J., Yao, Y., Wang, S., Sun, B., Ferguson, D. K., Li, C., Li, M.,
- Deng, T., and Wang, Y.: Palynological evidence reveals vegetation succession
- 986 in the central qinghai-tibet plateau during the late oligocene to early Mioce
- 987 ne, J. Syst. Evol., 63, 53-61, https://doi.org/10.1111/jse.13168, 2025.
- 988 Yang, Y., Nie, J., Miao, Y., Wan, S., and Jonell, T. N.: Tibetan Plateau uplift





989 and environmental impacts: New progress and perspectives, Front. Earth Sci., 990 10, 1020354, https://doi.org/10.3389/feart.2022.1020354, 2022. Zeng, S., Wang, J., Fu, X., Feng, X., and Wang, D.: Controls on organic matt 991 992 er enrichment of the early-middle miocene lacustrine oil shale, central tibet 993 (sw china): new insights from clay minerals and geochemistry, J. Asian Eart 994 h Sci., 262, 106007, https://doi.org/10.1016/j.jseaes.2024.106007, 2024. 995 Zhang, M., Guo, Z., Xu, S., Barry, P. H., Sano, Y., Zhang, L., Halldórsson, S. 996 A., Chen, A., Cheng, Z., Liu, C., Li, S., Lang, Y., Zheng, G., Li, Z., Li, L., 997 and Li, Y.: Linking deeply-sourced volatile emissions to plateau growth dyn 998 amics in southeastern Tibetan Plateau, Nat. Commun., 12, 4157, https://doi.or 999 g/10.1038/s41467-021-24415-y, 2021. 1000 Zhang, R., Jiang, D., Zhang, C., and Zhang, Z.: Distinct effects of Tibetan Pla 1001 teau growth and global cooling on the eastern and central Asian climates du 1002 ring the Cenozoic, Glob. Planet. Change, 218, 103969, https://doi.org/10.1016/ 1003 j.gloplacha.2022.103969, 2022. 1004 Zhang, Q., Zhang, J., Ma, C., Feng, Z., Tang, W., and Fang, X.: Tibetan plate 1005 au uplift changed the Asian climate and regulated its responses to orbital for cing during the late Eocene to early Miocene, J. Geophys. Res.-Atmos., 130, 1006 1007 e2024JD042872, https://doi.org/10.1029/2024JD042872, 2025. Zhao, Z., Lu, H., Wang, S., Li, H., Li, C., Liu, D., Pan, J., Zheng, Y., and B 1008 1009 ai, M.: The Cenozoic multiple-stage uplift of the Qiangtang Terrane, Tibetan





1010 plateau, Front. Earth Sci., 10, 818079, https://doi.org/10.3389/feart.2022.81807 1011 9, 2022. 1012 Zhou, K., Zhang, S., Yang, M., Lu, J., Gao, R., Tong, L., Yin, L., Zhang, P., 1013 Wang, W., Liu, H., Shao, L., Hilton, J.: Palaeoclimatic influence on lake pal 1014 aeoenvironment and organic matter accumulation in the Middle Jurassic Shim 1015 engou formation (Qaidam basin, NW China), Geoenergy Sci. Eng., 233, 212 581, https://doi.org/10.1016/j.geoen.2023.212581, 2024. 1016 1017 Zhu, Z., Chen, J. A., Zeng, Y., Li, H., Yan, H., and Ren, S.: Research on the 1018 carbon isotopic composition of organic matter from Lake Chenghai and Caoh ai Lake sediments, Chin. J. Geochem., 30, 107-113, https://doi.org/10.1007/s1 1019 1020 <u>1631-011-0491-9</u>, 2011. Zhu, Z., Chen, J., Zeng, Y.: Abnormal positive δ<sup>13</sup>C values of carbonate in La 1021 1022 ke Caohai, southwest China, and their possible relation to lower temperature, 1023 Quat. Int., 286, 85-93, https://doi.org/10.1016/j.quaint.2012.06.004, 2013. 1024 Zhuang, Q., Guo, M., Melack, J. M., Lan, X., Tan, Z., Oh, Y., and Leung, L. 1025 R.: Current and future global lake methane emissions: A process-based mode 1026 ling analysis, J. Geophys. Res-biogeo., 128, e2022JG007137, https://doi.org/10. 1027 1029/2022JG007137, 2023.